Magnetic Resonance in Medicine 55:296–301 (2006)

Proton MRS of the Unilateral Substantia Nigra in the Human Brain at 4 Tesla: Detection of High GABA Concentrations

Gülin Öz,[1*] Melissa Terpstra,[1] Ivan Tkáč,[1] Pratibha Aia,[2] Jodi Lowary,[2] Paul J. Tuite,[2] and Rolf Gruetter[1,3]

Parkinson's disease (PD) is characterized by loss of dopaminergic neurons in the substantia nigra (SN), the cause of which is unknown. Characterization of early SN pathology could prove beneficial in the treatment and diagnosis of PD. The present study shows that with the use of short-echo (5 ms) Stimulated-Echo Acquisition Mode (STEAM) spectroscopy and LCModel, a neurochemical profile consisting of 10 metabolites, including γ-aminobutyric acid (GABA), glutamate (Glu), and glutathione (GSH), can be measured from the unilateral SN at 4 tesla. The neurochemical profile of the SN is unique and characterized by a fourfold higher GABA/Glu ratio compared to the cortex, in excellent agreement with established neurochemistry. The presence of elevated GABA levels in SN was validated with the use of editing, suggesting that partial volume effects were greatly reduced. These findings establish the feasibility of obtaining a neurochemical profile of the unilateral human SN by single-voxel spectroscopy in small volumes. Magn Reson Med 55:296–301, 2006. © 2006 Wiley-Liss, Inc.

Key words: MRS; human; substantia nigra; GABA; Parkinson's disease

Parkinson's disease (PD) is characterized by loss of dopaminergic neurons in the substantia nigra (SN), but its etiology remains poorly understood. Mitochondrial dysfunction, oxidative stress, and glutamate (Glu) excitotoxicity may play roles in the pathogenesis of sporadic PD (1). However, evidence implicating these factors in PD has been limited to cell culture, animal model, and postmortem tissue studies. In vivo, positron emission tomography (PET) and single photon emission computed tomography (SPECT) have been used to distinguish patients with PD from normal controls (2), based on measures obtained from the striatum. Other in vivo methods are needed to assess the pathology of PD directly in the SN.

Neuronal loss of the SN can in principle be assessed by MRI (e.g., as indicated by atrophy of the structure). Interestingly, conventional MR images of patients with idiopathic PD are usually normal (3). A narrowing of the SN pars compacta (SN_{pc}), where most neuronal loss occurs in PD, has been reported in studies using MRI, albeit not consistently (4–8). Reduced water T_2 values have been observed in the SN, probably due to iron accumulation, with significant overlap between patients and controls (9). Recently developed inversion recovery techniques appear to be useful for visualizing nigral atrophy by utilizing a combination of two pulse sequences to suppress gray and white matter, respectively (10).

Magnetic resonance spectroscopy (MRS) potentially can detect pathogenic markers of PD that reflect metabolic, excitotoxic, and oxidative insults that likely occur before irreversible structural damage, such as changes in lactate (Lac), Glu, and glutathione (GSH) levels (11). Previous MRS studies of PD mostly reported ratios of NAA, creatine (Cr), and choline-containing compounds (Cho) (12,13). Decreased NAA/Cho or NAA/Cr ratios in PD were found in some studies (12,13). Most of these studies investigated the striatum or cortex. Because of its very small volume, the SN has been studied infrequently. Relatively large volumes of interest (VOIs; 3.4–8 ml) around the SN were employed in the few MRS studies that examined the unilateral or bilateral SN, resulting in partial volume effects (14–16). Since PD characteristically is an asymmetric condition, acquiring data from smaller VOIs encompassing the SN contralateral to the clinically first and more severely affected side of patients with PD is of interest.

In addition to its small size, other challenges of measuring MR spectra the SN include its location in the midbrain and its high iron content. Broader lines relative to other brain regions are expected in the SN, even with the use of automated shimming routines. However, increased sensitivity potentially can be achieved in the SN by utilizing a high magnetic field and an efficient volume coil. Spectra with higher information content can facilitate quantitation of neurotransmitters, such as Glu and γ-aminobutyric acid (GABA), and antioxidants, such as GSH, making it feasible to test pathogenic theories regarding PD.

The aims of the current study were to 1) demonstrate the feasibility of obtaining short-echo ^{1}H MR spectra at 4 T in small volumes encompassing the unilateral SN in healthy volunteers and patients with PD, and 2) determine which metabolites can be reliably quantified in these spectra.

[1]Center for MR Research, Department of Radiology, University of Minnesota, Minneapolis, Minnesota, USA.

[2]Department of Neurology, University of Minnesota, Minneapolis, Minnesota, USA.

[3]Department of Neuroscience, University of Minnesota, Minneapolis, Minnesota, USA.

Grant sponsors: Michael J. Fox Foundation; Minnesota Medical Foundation.

Pratibha Aia is now at the Department of Neurology, University of Arkansas for Medical Sciences, Little Rock, Arkansas, USA.

Rolf Gruetter is now at the Laboratory for Functional and Metabolic Imaging, Ecole Polytechnique Federale de Lausanne, Switzerland.

*Correspondence to: Gülin Öz, Center for MR Research, 2021 6th St. SE, Minneapolis, MN 55455. E-mail: gulin@cmrr.umn.edu

Received 4 May 2005; revised 26 August 2005; accepted 30 September 2005.
DOI 10.1002/mrm.20761
Published online 11 January 2006 in Wiley InterScience (www.interscience.wiley.com).

MATERIALS AND METHODS

Patients and Control Subjects

Ten patients with mild–moderate PD (six females and four males, 59 ± 10 years old, mean ± SD) and 11 age-matched healthy volunteers (seven females and four males, 59 ± 8 years old) were studied using stimulated-echo acquisition mode (STEAM) spectroscopy in 2.2-ml volumes centered on the unilateral SN. The Unified Parkinson's Disease Rating Scale (UPDRS) score for the patients was 27 ± 9 (mean ± SD), and the disease duration after diagnosis was 2.3 ± 1.5 years (mean ± SD). The patients were kept off their antiparkinsonian medications for at least 12 hr prior to the MR scan.

Additionally, five healthy volunteers (two females and three males, 28 ± 3 years old) studied with GABA editing were compared with four healthy volunteers (two females and two males, 29 ± 10 years old) studied with STEAM spectroscopy in 5.3-ml volumes encompassing the bilateral SN. All of the subjects were scanned after informed consent was obtained using procedures approved by the Institutional Review Board: Human Subjects Committee of the University of Minnesota.

STEAM Spectroscopy

All studies were performed on a 4 tesla, 90-cm bore magnet (Oxford Magnet Technology, Oxford, UK) with an INOVA console (Varian, Palo Alto, CA, USA) and a standard body gradient coil (Sonata, Siemens, Erlangen, Germany). A TEM volume coil was used as the NMR transceiver (17). After the subject was positioned in the magnet, transverse multislice images were obtained with a rapid acquisition with relaxation enhancement (RARE) sequence (repetition time (TR) = 4 s, echo train length = 8, echo spacing = 15 ms, echo time (TE) = 60 ms, seven slices, two averages) for selection of the VOI. Localization of ^1H MR spectra was achieved using ultrashort-echo STEAM spectroscopy with TE = 5 ms, mixing time (TM) = 42 ms, and TR = 4.5 s (18). Water suppression was achieved using eight variable power RF pulses with optimized relaxation delays (VAPOR) that were interleaved with outer volume suppression to improve localization performance (18). All first- and second-order shims were adjusted using Fast Automatic Shimming Technique by Mapping Along Projections (FASTMAP) with echo-planar readout (19). Spectra were acquired from a $1.3 \times 1.3 \times 1.3$ cm^3 volume (2.2 ml) to encompass the unilateral SN, and a $3.5 \times 1.5 \times 1.0$ cm^3 volume (5.3 ml) to encompass the SN bilaterally. The SN contralateral to the more affected side was selected in patients. Unavoidably, the 2.2-ml VOI contained parts of other brain structures, such as the red nucleus, subthalamic nucleus, and cerebral peduncle. However, this volume was selected as the smallest cubic volume around the SN because this structure extends rostrocaudally for 12 ± 2 mm in the human brain (20). In each VOI the unsuppressed water signal was obtained as a quantitation reference. The total time each volunteer spent in the magnet did not exceed 1 hr.

Spectral Quantitation

The contribution of individual metabolites to the in vivo spectrum was quantified using LCModel (21). The following 20 metabolites were included in the basis set: Alanine (Ala), aspartate (Asp), glycerophosphorylcholine (GPC), phosphorylcholine (PCho), creatine (Cr), phosphocreatine (PCr), GABA, glucose (Glc), glutamine (Gln), Glu, GSH, *myo*-inositol (*myo*-Ins), lactate (Lac), N-acetylaspartate (NAA), N-acetylaspartylglutamate (NAAG), phosphorylethanolamine (PE), *scyllo*-inositol (*scyllo*-Ins), taurine (Tau), and macromolecules (MM). The model metabolite spectra were obtained by simulation (18) using previously reported chemical shifts and coupling constants (22). The macromolecule pattern was obtained by averaging inversion recovery spectra from the right and left unilateral SNs (VOI = 2.2 ml) of five healthy subjects. For this measurement, the STEAM parameters were optimized to null the metabolite resonances (TR = 2 s, inversion time = 0.675 s). Since the signal-to-noise ratio (SNR) in this averaged spectrum was low, the macromolecule pattern was similarly obtained from the occipital gray matter (VOI = 8 ml) of five additional healthy subjects. Spectra were quantified by including both the occipital gray matter and the SN MM in the LCModel basis set for comparison. Quantification of the in vivo metabolite signals was based on the unsuppressed water signal obtained from the same voxel (23), assuming a water content of 82% (24).

Assessment of Reliability in Metabolite Concentrations and Statistical Analysis

The criteria for selecting the reliable metabolite concentrations were based on the Cramér-Rao lower bounds (CRLB), which are estimates of the %SD of the fit for each metabolite (21). Only results with a CRLB $\leq 50\%$ were included in the analysis. Concentrations with CRLB $> 50\%$ were classified as not detected. Only those metabolites that had a CRLB below 50% in at least half of the spectra were reported. If the covariance between two metabolites was consistently high (correlation coefficient < -0.5), such as in the case of Cr and PCr, their sum was reported rather than their individual values.

The concentrations of metabolites in controls and patients were compared using the two-tailed, unpaired Student's *t*-test, without a correction for multiple comparisons.

GABA Editing

To verify the GABA concentration obtained by STEAM spectroscopy, GABA editing was utilized. To provide sufficient SNR for edited spectroscopy, VOIs of 5.3 ml that encompassed the SN bilaterally were selected in healthy volunteers. MEGA-Point Resolved Spectroscopy (MEGA-PRESS) difference editing (TE = 68 ms, TR = 4.5 s) was optimized for detection of the $^4CH_2$ resonance of GABA (NH_2-$^4CH_2$-$^3CH_2$-$^2CH_2$-$^1CO_2H$) at 3.0 ppm via the coupled $^3CH_2$ resonance (1.9 ppm) with minimized signal contamination from MM, as described previously (25). Specifically, the offset of the editing pulse (20 ms Gaussian) alternated between 2.0 ppm (J-evolution suppressed, "on") and 1.4 ppm (J-evolution unsuppressed, "off") symmetrically around the coupling partner (1.7 ppm) of the 3.0 ppm MM resonance. Shifting the editing pulse from its ideal offset (1.9 ppm) to 2.0 ppm minimized loss of edited signal

via partial excitation of the $^3CH_2$ resonance by the "off" pulse. VAPOR water suppression and outer volume suppression preceded the MEGA-PRESS sequence. Each free induction decay (FID) (number of excitations (NEX) = 1) was frequency- and phase-corrected prior to summation as described previously (26). B_0 drift was <7 Hz, which ensured negligible MM contamination. All MEGA-PRESS pulse powers were calibrated on-resonance for water in a cerebrospinal fluid (CSF)-free subvolume of interest, where the water signal was sufficiently stable. Under this editing scheme, the ^2CH of Glu (3.74 ppm), Gln (3.75 ppm), and GSH (3.77 ppm) contributed a combined resonance via their coupling partners (~2.0–2.2 ppm) within the bandwidth of the editing pulse (2.0 ppm). NAA was used as an internal reference for quantitation of edited spectra as follows: An accordingly line-broadened MEGA-PRESS edited spectrum acquired from a phantom containing GABA (5 mM) and NAA (1 mM) was used to calibrate relative peak heights for quantitation of GABA. The NAA singlet at 2.01 ppm contributed to the edited spectrum via inversion on alternate scans. In vivo NAA concentration was set to that measured using LCModel analysis of corresponding short-echo STEAM spectra. Similarly, an edited spectrum from a phantom containing Glu (6 mM), Gln (2 mM), GSH (2 mM), and NAA (12 mM) was used to calibrate relative peak heights for quantitation of the combined Glu, Gln, and GSH resonance near 3.8 ppm. On the basis of prior studies (26), T_2 relaxation effects were assumed to have a negligible influence on quantitation.

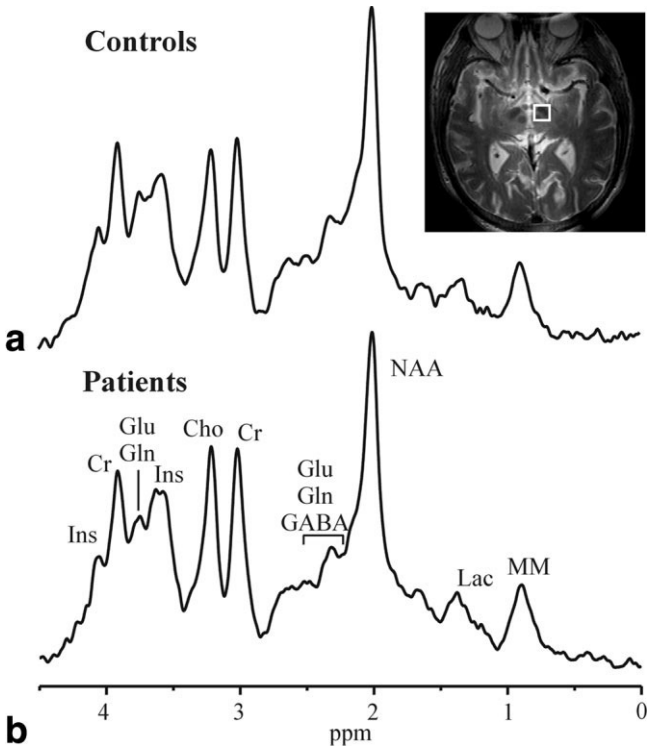

FIG. 1. Averaged ^1H MR spectra (TE = 5 ms, TR = 4.5 s, NEX = 400 for each subject) acquired from 2.2-ml volumes that encompass the SN of (**a**) 11 healthy volunteers and (**b**) 10 patients with PD. The typical VOI is shown in the T_2-weighted image.

RESULTS

Despite challenges in shimming and broad intrinsic linewidths relative to other brain areas, spectral quality that permitted assessment of the neurochemical profile of the SN was achieved in 2.2-ml volumes in single subjects. Spectral quality in patients with early PD and controls was similar (Fig. 1), based on the full width at half maximum (FWHM; 13.3 ± 2.1 Hz (mean ± SD) in controls, 13.5 ± 2.2 Hz in patients, $P = 0.9$) and SNR values (6.5 ± 0.8 in controls, 6.0 ± 1.2 in patients, $P = 0.3$) determined by LCModel. Similarly, the reliability of metabolite quantification with LCModel was comparable between the two groups (Fig. 2; see relative error bars in the patient and control groups). Of the 10 metabolites that met our criteria for reliable quantification (see Materials and Methods), four were quantified with a median CRLB (including all 21 spectra in the median determination) ≤ 10% (NAA + NAAG, Cr + PCr, and GPC + PCho (hereafter referred to as NAA, Cr, and Cho, respectively), and *myo*-Ins), two metabolites with a median CRLB of <30% (Glu and GSH), and three metabolites with a median CRLB of <40% (GABA, Glc + Tau, and *scyllo*-Ins) when the high-SNR gray matter MM spectrum was used in the LCModel basis set. The median CRLB for Lac was 50%. Using the SN MM spectrum did not change the neurochemical pattern; however, Lac was only quantified (CRLB ≤ 50%) in seven, and GABA in 10 of 21 spectra acquired from a 2.2-ml VOI in this case.

When the neurochemical profiles of the two groups were compared, Glu, NAA, and GSH showed a trend to decrease, and Cho showed a trend to increase in patients with PD (*P*-values obtained using gray matter and SN MM patterns were in the range of 0.1–0.2 for all of these metabolites; Fig. 2a). To ensure that the quality of individual spectra was sufficient to accurately assess these trends, averaged spectra from the patient and control groups were quantified identically and showed the same trends (Fig. 2b).

Two of the concentrations determined in SN (high GABA and low Glu) were very different from those in the occipital cortex ($P < 0.00001$; Fig. 2a). To investigate whether these differences were an effect of linewidth and low SNR, the occipital cortex spectra of four averages were line-broadened and appropriate amounts of noise were added to these spectra to mimic the spectral quality of the SN spectra (linewidth and SNR). Glu concentrations estimated with LCModel showed a trend to decrease when the linewidth was increased and SNR decreased, indicating that the reported Glu levels in the SN may be underestimated. GABA became undetectable (CRLB > 50%) in about half of the spectra, indicating that the high values observed in the SN were not a result of broad lines and low SNR. Overall, the changes did not explain the drastically (fourfold) different GABA/Glu ratios observed in SN vs. cortex.

To further substantiate the presence of an elevated GABA/Glu ratio, averaged spectra from both subject groups were inspected (Fig. 3). Clearly, the peak at 2.32 ppm in the averaged spectrum is between the 2.34 ppm $^4CH_2$ resonance of Glu and the 2.28 ppm $^2CH_2$ resonance of GABA, indicating that Glu and GABA contribute comparably to the spectrum.

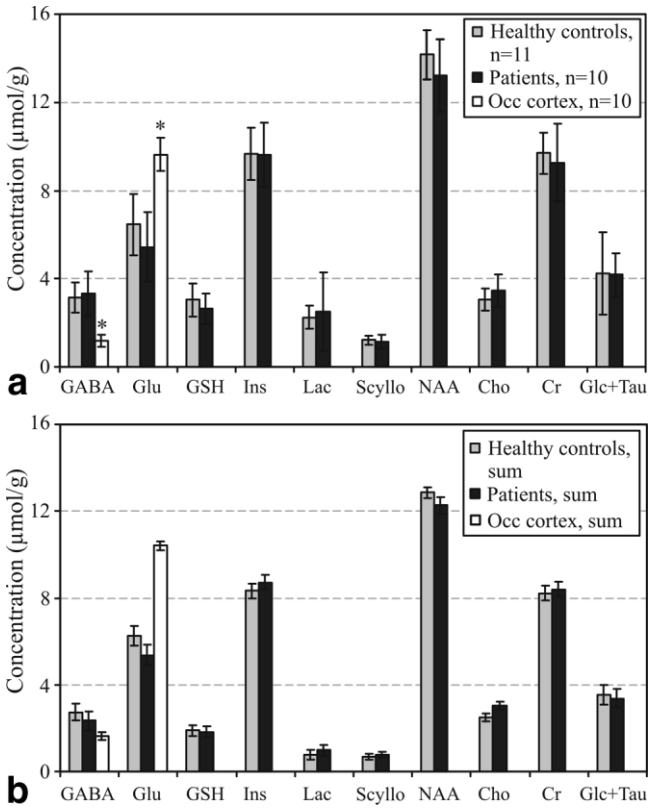

FIG. 2. Metabolite concentrations determined by LCModel fitting of (**a**) individual and (**b**) averaged STEAM spectra from the SN of controls and patients with PD (VOI = 2.2 ml, gray matter macromolecule pattern utilized). Also shown are the GABA and Glu concentrations obtained in the occipital cortex (VOI = 8 ml) of 10 healthy volunteers. The errors shown in a are SDs, and in b CRLB obtained from LCModel. * $P < 0.00001$ occipital cortex vs. SN of both controls and patients.

To further verify the quantification of GABA, MEGA-PRESS editing was utilized in VOIs that encompassed the SN bilaterally (Fig. 4). The edited GABA resonance (3.0 ppm) was detected in all five volunteers scanned. The in vivo GABA concentration was estimated from each of the five edited spectra relative to 11 μmol/g NAA, the average NAA concentration measured from STEAM spectra acquired in 5.3-ml voxels. The GABA concentration measured using STEAM (2.4 ± 0.4 μmol/g, mean ± SD) in four healthy volunteers from the same VOI was in excellent agreement with the editing (2.4 ± 0.5 μmol/g). At 4 T, resonances from Glu, Gln, and GSH coedited with and were well resolved from GABA (Fig. 4). The sum of their concentrations in vivo was estimated at 8.7 μmol/g from the combined edited resonance at 3.76 ppm, in good agreement with the 8.4 μmol/g of Glu + Gln + GSH measured from the same VOI using STEAM and LCModel analysis.

To compare edited GABA quantitation in the SN with that in the occipital cortex, we acquired an edited GABA spectrum from a 27-ml VOI in one volunteer (Fig. 4b). Relative to the summed SN spectrum acquired from a 5.3-ml VOI and averaged over five volunteers, the sensitivity in this spectrum was more than doubled. Indeed, the cortical GABA peak was much smaller than the SN GABA peak and corresponded to a GABA concentration of <1 μmol/g, in agreement with literature (25).

DISCUSSION

We have demonstrated the feasibility of obtaining short-echo STEAM spectra and assessing the neurochemical profile from small volumes in the midbrain encompassing the SN, an area of interest in PD. Upon LCModel fitting of spectra from healthy volunteers and patients with PD, 10 metabolites were quantified reliably and included in the neurochemical profile. This profile was unique to the SN region with high GABA and low Glu levels. The high GABA concentration was verified by editing for this metabolite, since in short-echo STEAM spectra resonances from GABA are overlapped with resonances from other neurochemicals, such as Cr and Glu.

LCModel fitting of individual STEAM spectra (VOI = 2.2 ml) resulted in the same neurochemical pattern obtained by fitting of averaged spectra (Fig. 2), indicating adequate spectral quality for reliable quantification in individual volunteers. With the use of this small VOI, partial volume effects were reduced compared to previous MRS studies of the SN. Better localization in the SN potentially can be achieved by utilizing oblique voxels, as well as multiple spatial saturation planes to define the noncuboidal shape of the SN, as recently proposed (27). However, uncertainties pertaining to the definition of the borders of SN in T_2-weighted images exist (8). The 2.2-ml volume we chose included the entire structure beyond these uncertainties.

The reduction in partial volume effects was further supported by the high GABA and low Glu levels detected in the neurochemical profile obtained from both individual and averaged spectra (Figs. 2 and 3). Note that the GABA moiety of homocarnosine may partially contribute to the free GABA signal (25), since the homocarnosine concen-

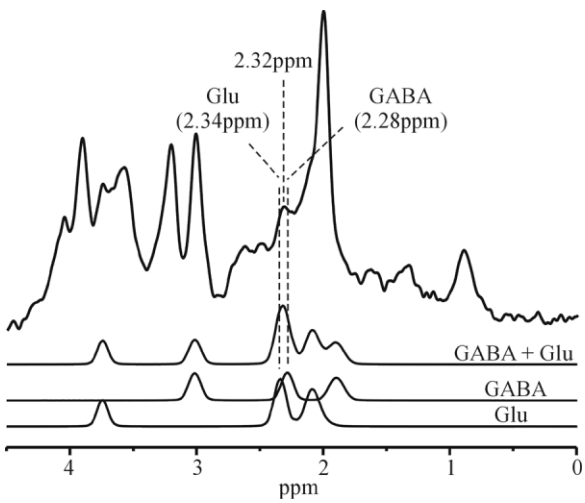

FIG. 3. Validation of high GABA concentrations in averaged spectra from healthy controls (N = 11, VOI = 2.2 ml). Below the averaged spectrum are shown the contributions of GABA and Glu, as well as their sum, to the in vivo spectrum as determined by LCModel. The 2.32 ppm peak clearly lines up with the summed contributions of GABA and Glu.

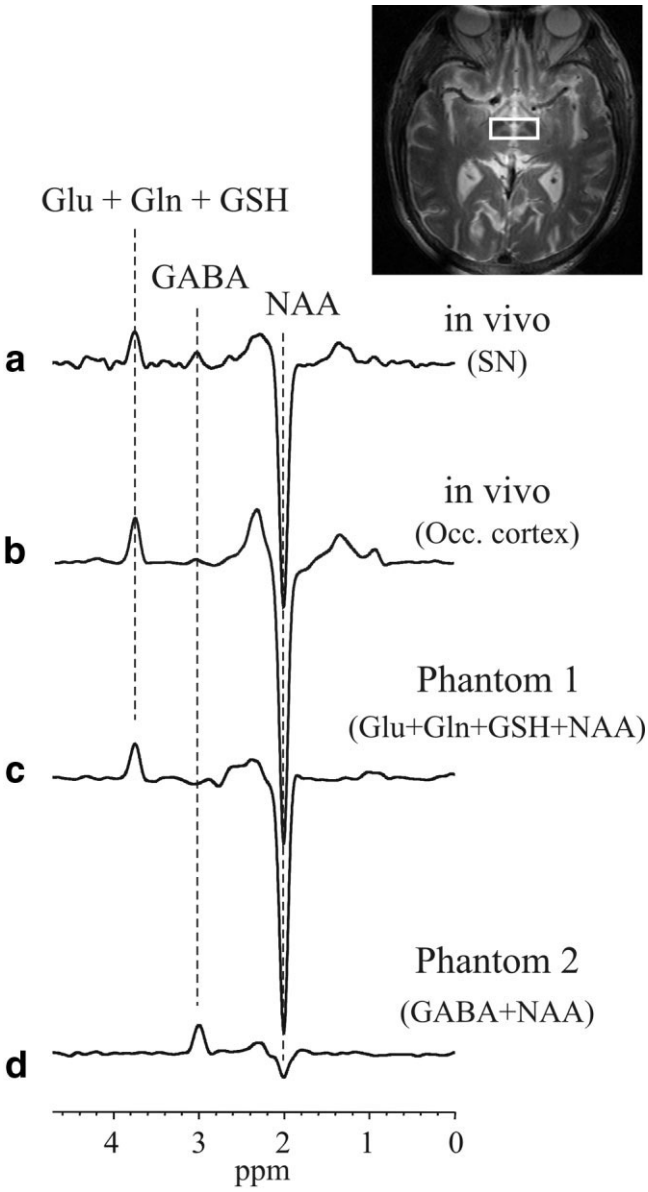

FIG. 4. MEGA-PRESS edited spectra (TE = 68 ms, TR = 4.5 s) acquired from (**a**) an in vivo VOI of 5.3 ml (NEX = 512 in each subject, averaged over five subjects) encompassing the SN, illustrated on T_2-weighted image; (**b**) an in vivo VOI of 27 ml ($3 \times 3 \times 3$ cm^3) located in the occipital cortex (NEX = 512 in one subject) and accordingly line-broadened; (**c**) a phantom containing 6 mM Glu, 2 mM Gln, 2 mM GSH, and 12 mM NAA (NEX = 512, VOI = 5.3 ml) and accordingly line-broadened; and (**d**) a phantom containing 5 mM GABA and 1 mM NAA (NEX = 512, VOI = 5.3 ml) and accordingly line-broadened. The spectra were scaled based on the NAA peak height and concentration.

tration is about one-third that of GABA in the cortex. However, the homocarnosine-to-GABA concentration ratio in the SN is approximately half of that in the cortex (28), and therefore this contribution is expected to be smaller in the SN. High GABA levels in the SN have been documented in postmortem human and animal brains (28–30). The absolute GABA concentration we obtained from the 2.2-ml VOI (3.2 μmol/g) was less than that measured in the autopsied human brain (5–6 μmol/g) (28,29), likely because of the well-known postmortem increase of GABA in the brain. On the other hand, the ratio of GABA levels in SN vs. cortex (~3×) observed in the current study were the same as in postmortem brain (28–30).

The difficulty of GABA quantitation was underscored by the effect of including different macromolecule spectra in the LCModel basis. Inclusion of the noisy SN macromolecule pattern resulted in reduced reliability of quantitation of this neurotransmitter. Nevertheless, the GABA quantification by STEAM spectroscopy was substantiated by MEGA-PRESS editing for GABA. Based on the edited GABA spectrum acquired from a 27-ml volume in the occipital cortex (Fig. 4b), the low (~1 μmol/g) GABA concentrations typical of other brain regions would not have been detected in 5.3-ml volumes in individual edited spectra (NEX = 512). The fact that GABA was detected in all five edited spectra is evidence of an elevated GABA concentration in the region encompassing the SN. In addition, the GABA concentrations quantified from edited and STEAM spectra were very similar, indicating that LCModel analysis of short-echo STEAM spectra acquired from the SN at 4 T provides accurate quantitation of GABA, despite overlapping resonances. The GABA concentration acquired from the 5.3-ml VOI (2.4 μmol/g) was less than what was measured in the 2.2-ml VOI (3.2 μmol/g), as was the case with all other metabolites. This was expected due to the higher partial volume effect from CSF in the center of this larger volume. The 2.2-ml volume did not contain CSF based on images. Additionally, based on a series of water signals acquired from this volume at different TE values (5–1200 ms), we did not detect a long T_2 component of the exponential decay of the water signal with increasing TE, which also indicates a negligible CSF contribution.

The few published MRS studies of the SN in PD utilized larger volumes encompassing the SN (3.4–8 ml). Choe et al. (14) observed a laterality of the NAA/Cr ratio between asymptomatic and symptomatic sides of SN in PD, and Baik et al. (16) detected a decrease in NAA/Cho after thalamotomy. When O'Neill et al. (15) compared the SN spectra of patients and controls, they observed decreased Cr in patients with bilateral symptoms of at least moderate severity. With the limited number of patients scanned in the current study, we observed trends in Glu, NAA, GSH, and Cho in patients relative to controls. These trends were not a result of different degrees of spectral quality achieved in the patient and control groups, since similar linewidths and SNRs were observed in the two groups. In this preliminary account, the patient group was scanned merely to establish feasibility, and the only criterion for inclusion in the study was a diagnosis of PD within the last 5 years. Therefore, heterogeneity in this small patient group may have obscured more decisive observations.

PD has a preclinical period of 4–6 years (3) and early detection of this disorder is of high interest in light of the neuroprotective agents that are being tested in clinical trials (31). Identification of pathogenic markers of PD in the SN could not only enable early detection of this disease, but could also improve our understanding of the causes of neuronal loss in this region and aid in monitoring the effects of potential neuroprotective agents. The

potential of MRS in this area is further underlined by anticipated increases in sensitivity. Thus, the utilization of even higher magnetic fields is expected to enable further reductions of the VOI and to increase the sensitivity to detect potential biochemical changes associated with neuronal loss in the SN_{pc}. For example, the use of a 7 tesla magnet along with a PRESS-type sequence instead of STEAM can result in an up to fourfold sensitivity increase in the same VOI. Alternatively, the sensitivity in the current study potentially can be reached in VOIs of ~0.5–0.6 ml.

In conclusion, single-voxel spectroscopy of the unilateral human SN is feasible in both healthy volunteers and patients with PD. This technique provides an in vivo neurochemical profile that includes neurotransmitter (Glu and GABA) and antioxidant (GSH) levels that are in excellent agreement with neurochemistry literature.

ACKNOWLEDGMENTS

We thank the staff of the Center for MR Research for maintaining and supporting the NMR system. The Center for MR Research is supported in part by the MIND Institute and National Center for Research Resources (NCRR) biotechnology research resource grant P41RR08079. The General Clinical Research Center at the University of Minnesota is supported by NCRR grant M01RR00400. This research was supported by grants from the Michael J. Fox Foundation (R.G.) and the Minnesota Medical Foundation (P.J.T.).

REFERENCES

1. Schapira AH. Causes of neuronal death in Parkinson's disease. Adv Neurol 2001;86:155–162.
2. Hu MT, White SJ, Herlihy AH, Chaudhuri KR, Hajnal JV, Brooks DJ. A comparison of ^{18}F-dopa PET and inversion recovery MRI in the diagnosis of Parkinson's disease. Neurology 2001;56:1195–1200.
3. Brooks DJ. Morphological and functional imaging studies on the diagnosis and progression of Parkinson's disease. J Neurol 2000;247(Suppl 2):II11–II18.
4. Duguid JR, De La Paz R, DeGroot J. Magnetic resonance imaging of the midbrain in Parkinson's disease. Ann Neurol 1986;20:744–747.
5. Stern MB, Braffman BH, Skolnick BE, Hurtig HI, Grossman RI. Magnetic resonance imaging in Parkinson's disease and parkinsonian syndromes. Neurology 1989;39:1524–1526.
6. Pujol J, Junque C, Vendrell P, Grau JM, Capdevila A. Reduction of the substantia nigra width and motor decline in aging and Parkinson's disease. Arch Neurol 1992;49:1119–1122.
7. Adachi M, Hosoya T, Haku T, Yamaguchi K, Kawanami T. Evaluation of the substantia nigra in patients with parkinsonian syndrome accomplished using multishot diffusion-weighted MR imaging. AJNR Am J Neuroradiol 1999;20:1500–1506.
8. Oikawa H, Sasaki M, Tamakawa Y, Ehara S, Tohyama K. The substantia nigra in Parkinson disease: proton density-weighted spin-echo and fast short inversion time inversion-recovery MR findings. AJNR Am J Neuroradiol 2002;23:1747–1756.
9. Antonini A, Leenders KL, Meier D, Oertel WH, Boesiger P, Anliker M. T_2 relaxation time in patients with Parkinson's disease. Neurology 1993;43:697–700.
10. Hutchinson M, Raff U. Structural changes of the substantia nigra in Parkinson's disease as revealed by MR imaging. AJNR Am J Neuroradiol 2000;21:697–701.
11. Öz G, Tkáč I, Charnas LR, Choi IY, Bjoraker KJ, Shapiro EG, Gruetter R. Assessment of adrenoleukodystrophy lesions by high field MRS in non-sedated pediatric patients. Neurology 2005;64:434–441.
12. Clarke CE, Lowry M. Systematic review of proton magnetic resonance spectroscopy of the striatum in parkinsonian syndromes. Eur J Neurol 2001;8:573–577.
13. Firbank MJ, Harrison RM, O'Brien JT. A comprehensive review of proton magnetic resonance spectroscopy studies in dementia and Parkinson's disease. Dement Geriatr Cogn Disord 2002;14:64–76.
14. Choe BY, Park JW, Lee KS, Son BC, Kim MC, Kim BS, Suh TS, Lee HK, Shinn KS. Neuronal laterality in Parkinson's disease with unilateral symptom by in vivo ^{1}H magnetic resonance spectroscopy. Invest Radiol 1998;33:450–455.
15. O'Neill J, Schuff N, Marks Jr WJ, Feiwell R, Aminoff MJ, Weiner MW. Quantitative ^{1}H magnetic resonance spectroscopy and MRI of Parkinson's disease. Mov Disord 2002;17:917–927.
16. Baik HM, Choe BY, Son BC, Jeun SS, Kim MC, Lee KS, Kim BS, Lee JM, Lee HK, Suh TS. Proton MR spectroscopic changes in Parkinson's diseases after thalamotomy. Eur J Radiol 2003;47:179–187.
17. Vaughan JT, Hetherington HP, Otu JO, Pan JW, Pohost GM. High frequency volume coils for clinical NMR imaging and spectroscopy. Magn Reson Med 1994;32:206–218.
18. Tkáč I, Gruetter R. Methodology of ^{1}H NMR spectroscopy of the human brain at very high magnetic fields. Appl Magn Reson 2005; 29:139–157.
19. Gruetter R, Tkáč I. Field mapping without reference scan using asymmetric echo-planar techniques. Magn Reson Med 2000;43:319–323.
20. Hardman CD, Henderson JM, Finkelstein DI, Horne MK, Paxinos G, Halliday GM. Comparison of the basal ganglia in rats, marmosets, macaques, baboons, and humans: volume and neuronal number for the output, internal relay, and striatal modulating nuclei. J Comp Neurol 2002;445:238–255.
21. Provencher SW. Estimation of metabolite concentrations from localized in vivo proton NMR spectra. Magn Reson Med 1993;30:672–679.
22. Govindaraju V, Young K, Maudsley AA. Proton NMR chemical shifts and coupling constants for brain metabolites. NMR Biomed 2000;13: 129–153.
23. Kreis R, Ernst T, Ross BD. Absolute quantitation of water and metabolites in the human brain. II. Metabolite concentrations. J Magn Reson 1993;102:9–19.
24. Siegel GJ, editor. Basic neurochemistry: molecular, cellular and medical aspects. 6th ed. Philadelphia: Lippincott-Raven Publishers; 1999.
25. Terpstra M, Uğurbil K, Gruetter R. Direct in vivo measurement of human cerebral GABA concentration using MEGA-editing at 7 Tesla. Magn Reson Med 2002;47:1009–1012.
26. Terpstra M, Henry PG, Gruetter R. Measurement of reduced glutathione (GSH) in human brain using LCModel analysis of difference-edited spectra. Magn Reson Med 2003;50:19–23.
27. Ryner L, Westmacott G, Davison N, Latta P. Automated positioning of multiple spatial saturation planes for non-cuboidal voxel prescription in MR spectroscopy. In: Proceedings of the 13th Annual Meeting of ISMRM, Miami Beach, FL, USA, 2005. p 350.
28. Perry TL. Cerebral amino acid pools. In: Lajtha A, editor. Handbook of neurochemistry. 2nd ed, Vol. 1. New York: Plenum Press; 1982. p 166.
29. Urquhart N, Perry TL, Hansen S, Kennedy J. GABA content and glutamic acid decarboxylase activity in brain of Huntington's chorea patients and control subjects. J Neurochem 1975;24:1071–1075.
30. Wasterlain CG, Baxter CF, Baldwin RA. GABA metabolism in the substantia nigra, cortex, and hippocampus during status epilepticus. Neurochem Res 1993;18:527–532.
31. Clarke CE. Neuroprotection and pharmacotherapy for motor symptoms in Parkinson's disease. Lancet Neurol 2004;3:466–474.